Critical behaviour of a kinetic gelation model with a constant initiator creation rate

1989 J. Phys. A: Math. Gen. 22 4695

(http://iopscience.iop.org/0305-4470/22/21/031)

J. Phys. A: Math. Gen. **22** (1989) 4695-4705. Printed in the UK

Critical behaviour of a kinetic gelation model with a constant initiator creation rate

D Matthews-Morgan† and D P Landau

Center for Simulational Physics, University of Georgia, Athens, GA 30602, USA

Received 24 October 1988, in final form 27 February 1989

Abstract. We present results from a computer simulation study of a radical initiated kinetic growth model in which the radicals (initiators) are created with a constant rate r_c. Simulations of the growth process were carried out on simple cubic lattices as large as $100 \times 100 \times 100$ for two values of the initiator creation rate. Finite-size scaling analyses of the bulk properties yield critical exponents which are the same, to within error bars, as those found in similar kinetic gelation models and in percolation studies. The critical amplitude ratio C^-/C^+ is consistent with the values obtained in the kinetic gelation studies with fixed initiator concentrations but is clearly different from percolation values. The cluster size distribution shows the same monotonic behaviour as seen in percolation and is markedly different from the oscillatory behaviour seen in an investigation of a similar gelation model. The scaling properties of the cluster size distribution, however, cannot be described using simple droplet theory. Instead, we use a generalised scaling form which produces a good fit to the cluster data.

1. Introduction

In recent years considerable effort [1-12] has been concentrated on the study of models for irreversible gelation in which an infinite macromolecule (gel) is formed by the joining of a collection of smaller macromolecules (sol). This sol-gel transition was first described theoretically by Flory [1] and Stockmayer [2], who used a simple model for percolation on a Cayley tree. DeGennes [3] and Stauffer [4] later drew the analogy between gelation and critical-point behaviour and suggested that percolation on a real lattice would provide a more realistic description of the sol-gel transition. However, realistic gelation processes, such as addition polymerisation in which macromolecules are formed through the crosslinking of linearly growing polymers, involve kinetic aspects in the formation of macromolecules. This kinetic gelation process has been extensively studied through computer simulations [5-12].

One major goal in studies of kinetic gelation models has been to determine how the physical parameters of a given model affect its critical behaviour. For example, Herrmann *et al* [6] have extensively studied a three-dimensional model for addition polymerisation in which polymer clusters are grown from a fixed initial concentration of radicals (initiators). Their results indicate that changes in the initiator concentration affect the universality class of the model, whereas monomer functionality, i.e. the number of available bonds per monomer, does not. The universality class is determined

† Present address: Advanced Computational Methods Center, University of Georgia, Athens, GA 30602, USA.

0305-4470/89/214695+11$02.50

by the values of various critical exponents and possibly critical amplitude ratios. Other three-dimensional studies [7–9] suggest that poison seems to affect universal properties, whereas solvent molecules, monomer mobility and chain-preferred reactions do not. Investigations [10, 11] of cluster size distributions in three-dimensional gelation models also support the notion that kinetic gelation belongs to a universality class different from percolation, showing non-monotonic behaviour in the cluster distributions compared with the monotonic distributions seen in percolation [13].

To further investigate the effects of different physical processes on kinetic gelation models, we have studied an irreversible, kinetic gelation model in three dimensions in which initiators are created with a constant rate r_c. A similar model, which produces initiators to keep the concentration of non-trapped, non-annihilated initiators fixed throughout the growth process, has been investigated by Pandey [7] using computer simulations. His investigation, however, differs from ours in that the initiator concentration in our model increased during the growth process and our initiators were created in a different manner. In addition, Pandey's study was not concerned with critical phenomena.

It is important to emphasise that our model is the same as that studied by others (see references in [11]), except for the additional kinetic aspects associated with the creation of initiators at different times in the growth process. We consider growth processes in which the timescale for creating initiators is roughly the same as the timescale for forming bonds. In the model described in [5, 6], the timescale for the creation of initiators is essentially zero compared with the timescale for the formation of bonds. Conservation of the number of initiators throughout the growth process [7] corresponds to steady-state conditions in polymer formation.

In the following section we describe the model and details of the computer simulations, and we provide a brief theoretical description of the analyses used in the study. Section 3 contains the analyses of bulk properties and cluster size distributions and a discussion of the results. A summary of our conclusions can be found in § 4.

2. Background

2.1. Model and simulation method

Our model consists of four-functional monomers positioned on the sites of an $L \times L \times L$ simple cubic lattice with periodic boundary conditions. Growth of polymer clusters begins with the creation of initiators (radicals with one unsaturated bond) at a constant rate r_c. This rate is defined as the probability per unit time of creating an initiator. In this model, one unit of time t_0 is defined as an attempt to create an initiator; r_c will henceforth be given in units of t_0^{-1}.

Once an initiator is created, its unsaturated bond is filled by satisfying one bond of a chemical double bond in a monomer and leaving the other bond unsatisfied. This unsatisfied bond (active centre) is then free to react with an available nearest neighbour. After each attempt has been made to create an initiator with probability $r_c t_0$, an attempt is made to form a bond between an active centre and a neighbouring monomer site. Figure 1 shows a snapshot of the growth process for several time steps. As one can see from this figure, a number of initiators have been created after time t_1 has elapsed, and many of the active centres produced by these initiators have formed bonds between neighbouring monomers. After times t_2 and t_3, additional active centres have been

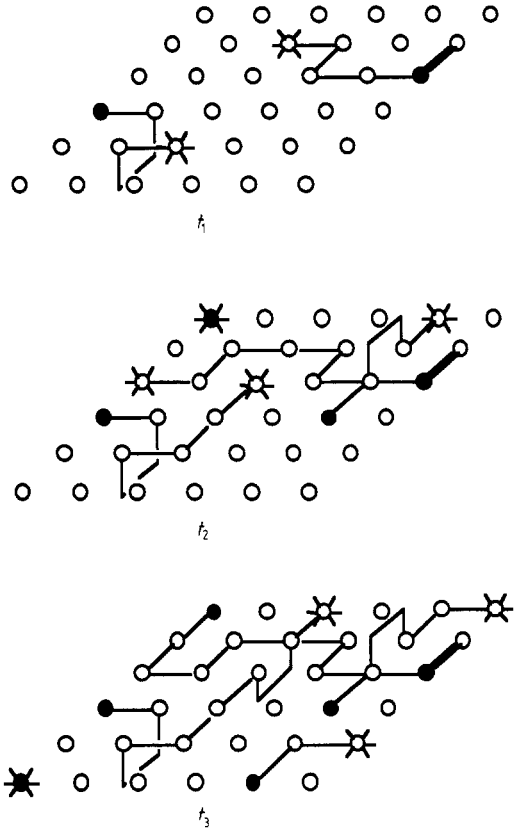

Figure 1. Schematic view of growth within a single layer after simulation time steps t_1, t_2 and t_3. Open circles represent tetrafunctional monomers and full circles represent monomers that have initiators bonded to them. Starred circles indicate the current position of active centres. Bonds, represented by lines between monomers, include those formed with adjacent layers.

produced by the creation of new initiators (some of these form new monomer clusters), and additional monomer bonds have been formed from these active centres.

The algorithm used for bond formation between monomers starts by randomly choosing an active centre and one of its nearest-neighbour (NN) sites. If the NN site is not fully occupied, a bond is formed between the sites. The new site then becomes the active centre, provided it was not one to begin with, since it now has an unsatisfied bond. Propagation of an active centre terminates when it bonds with another active centre (annihilation) or when all of its neighbours are inaccessible (trapping).

After a specified number of bonds have been formed, we calculate the chemical conversion factor p (defined as the fraction of total possible bonds already formed), the number of clusters n_s containing s monomer sites, the average molecular weight or 'susceptibility'

$$\chi = \sum_s s^2 n_s \tag{1}$$

and the gel fraction

$$G = 1 - \sum_s s n_s. \tag{2}$$

The sums in (1) and (2) exclude the largest cluster (macromolecule). Averages for the cluster numbers, the susceptibility, and the gel fraction are taken over several samples, i.e. different starting positions for the initiators created with rate r_c.

In an infinite system G is zero for all p up to the gel point p_c; for $p > p_c$ the gel fraction grows as

$$G = B^+ \mathscr{P}'^{\beta} \tag{3}$$

with $\mathscr{P}' = (p - p_c)/p_c$. In the vicinity of p_c the susceptibility also shows critical behaviour of the form

$$\chi p = \begin{cases} C^- \mathscr{P}^{-\gamma} & p < p_c \quad (4a) \\ C^+ \mathscr{P}'^{-\gamma} & p > p_c \quad (4b) \end{cases}$$

where $\mathscr{P} = (p_c - p)/p$, C^- is the critical amplitude below p_c and C^+ is the amplitude above p_c. The ratio of critical amplitudes is defined as $R = C^-/C^+$. The correlation length ξ diverges at p_c as

$$\xi = \xi_0 \mathscr{P}'^{-\nu}. \tag{5}$$

In most polymerisation processes the initiator creation rate is small in comparison with the bond formation rate [14] and, therefore, we have limited the creation rates under investigation to small values. We have chosen two rates, namely $r_c = 0.005$ and $r_c = 0.05$, in order to maintain a low creation rate yet still enable us to make comparisons between rates which differ by an order of magnitude. The analyses were performed on lattices with L between 14 and 100; the number of samples used in the averages ranged from 800 to 10,000.

2.2. *Finite-size scaling*

In an infinite system, the susceptibility diverges at the gel point, which corresponds to an infinite correlation length ξ. For finite lattices, the susceptibility deviates from infinite lattice behaviour, e.g. it has a finite peak at p_c when ξ is larger than the system size L. Data obtained for finite lattices can be related to the corresponding infinite lattice singularities through the use of finite-size scaling theory. This approach, first developed for thermal phase transitions [15], expresses bulk quantities of $L \times L \times L$ systems in terms of homogeneous scaling functions of a variable $x = \mathscr{P} L^{1/\nu}$ or $x = \mathscr{P}' L^{1/\nu}$. For the 'susceptibility' the form which we use is

$$\chi p = L^{\gamma/\nu} f(x) \tag{6}$$

where $f(x)$ is a scaling function. For the gel fraction the appropriate form is

$$G = L^{-\beta/\nu} g(x). \tag{7}$$

(These scaling forms are valid asymptotically for large L.) Thus by making double logarithmic plots of $\chi p L^{-\gamma/\nu}$ against x and $GL^{\beta/\nu}$ against x, we can vary p_c and the critical exponents until the data collapse onto single curves (one curve for $p < p_c$ and one for $p > p_c$) defining $f(x)$ and $g(x)$, respectively. In addition, the behaviour of (6) and (7) must correctly reproduce the infinite lattice critical behaviour in the limit that $L \to \infty$. This restriction requires that

$$f(x) \to x^{-\gamma} \qquad x \to \infty \tag{8a}$$

$$g(x) \to x^{\beta} \qquad x \to \infty, p > p_c \tag{8b}$$

and the scaling plots must obey this restriction as a consistency check.

2.3. Droplet scaling theory

As bonds are formed in the system a distribution of clusters results in which each cluster is composed of a collection of sites which are connected to each other at least once by an unbroken string of bonds. This situation is similar to that which occurs for thermal transitions where 'droplets' of ordered material form. The bulk properties for these transitions have been described in terms of a droplet theory proposed by Essam and Fisher [16] and used by Stauffer [17] to analyse random percolation. In terms of our variables the cluster size distribution $n_s(p)$, which gives the number of clusters of size s, should have the following behaviour near p_c:

$$n_s(p) = s^{-\tau} f(|p - p_c| s^{\sigma}). \tag{9}$$

The moments of this distribution can also be related to bulk properties. For example, the second moment of $n_s(p)$ yields the critical behaviour of the susceptibility through

$$\chi = \sum_s s^2 n_s \sim |(1 - p/p_c)|^{-\gamma}. \tag{10}$$

3. Results and discussion

3.1. Bulk properties

The 'susceptibility' χ and the gel fraction G, near the gel point p_c, were investigated as a function of chemical conversion factor p and lattice size L. Figure 2 shows plots of χ against p for two initiator creation rates r_c. Stronger finite-size effects can be seen in the plot corresponding to the smaller creation rate $r_c = 0.005$ when compared with the larger rate $r_c = 0.05$. The peak in the susceptibility for $r_c = 0.05$ is roughly five times larger than the peak for $r_c = 0.005$ when comparing data for the same lattice size. There is also a large shift in the effective gel point $p_c(L)$ for a given lattice size L for the smaller value of r_c and very little shift in $p_c(L)$ for the large creation rate. Similar finite-size effects are seen in plots of G against p for both values of r_c, as shown in figure 3. Pronounced finite-size effects were also seen in a similar kinetic gelation

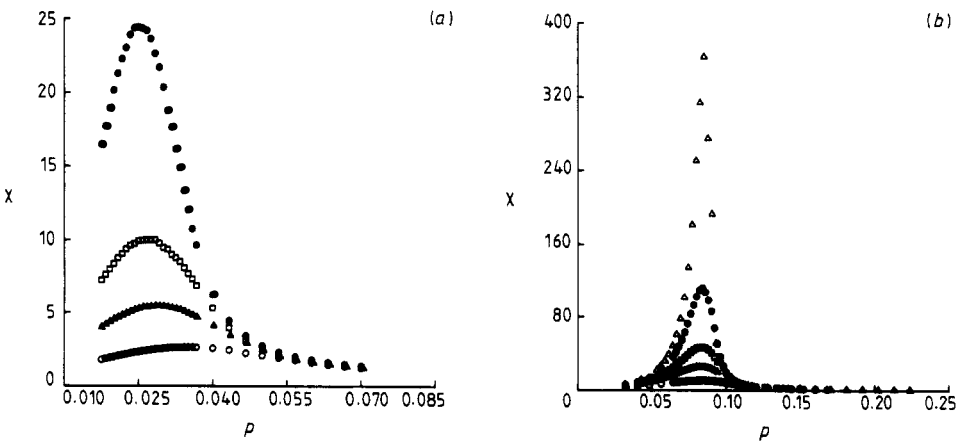

Figure 2. Susceptibility (second moment of the cluster size distribution) χ as a function of p for two values of r_c: (*a*) $r_c = 0.005$, (*b*) $r_c = 0.05$. Curves are shown for several different values of L: 20(○), 30(▲), 40(□), 60(●) and 100(△).

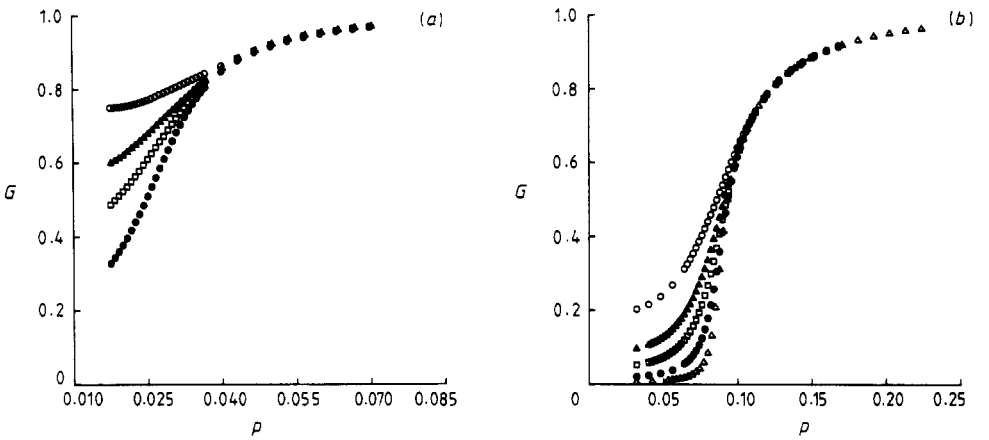

Figure 3. Gel fraction G as a function of p for two values of r_c: (a) $r_c = 0.005$, (b) $r_c = 0.05$. Curves are shown for several different values of L: 20(○), 30(▲), 40(□), 60(●) and 100(△).

study by Chhabra *et al* [11]. These effects became more evident as the initiator concentration c_I decreased. Our results are consistent with these findings since the effective initiator concentration, proportional to the number of initiators present, at p_c is smaller for $r_c = 0.005$ than for $r_c = 0.05$.

Finite-size scaling [6, 15] analyses are used to determine the critical exponents β, γ and ν, the critical amplitude ratio R, and the gel point p_c. By plotting $\chi pL^{-\gamma/\nu}$ against the scaling variable x one varies the parameters γ, ν and p_c until the data for every lattice size fall onto a single, universal curve representing the function $f(x)$ in (6). Figure 4 shows an optimal fit of the scaled susceptibility data for $r_c = 0.05$ which

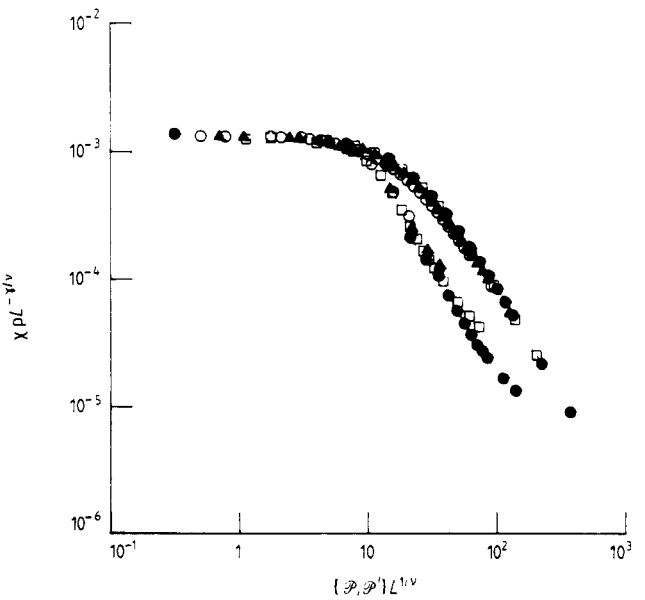

Figure 4. Finite-size scaling plot for the susceptibility χ for $r_c = 0.05$, $p_c = 0.0852$, $\gamma = 1.85$ and $\nu = 0.85$. Curves are shown for several values of L: 30(○), 40(▲), 60(□) and 100(●).

yield parameter estimates of $\gamma = 1.8 \pm 0.1$, $\nu = 0.80 \pm 0.07$ and $p_c = 0.0850 \pm 0.0007$. These values for γ and ν are consistent with those found in a similar gelation model [6, 8, 11] as well as percolation values [17]. Errors are estimated by finding the range of parameter values which gives a reasonable fit to the data. Deviations from the universal curve farther away from p_c, i.e. larger values of x, are due to corrections to scaling.

Similar procedures are carried out for the gel fraction by plotting $GL^{\beta/\nu}$ against x and varying β, ν and p_c until the universal curve $g(x)$, defined through (7), is obtained. For initiator creation rate $r_c = 0.05$, we obtain a best fit of the scaled gel fraction, shown in figure 5, with the parameters $\beta = 0.40 \pm 0.07$, $\nu = 0.80 \pm 0.06$ and $p_c = 0.0850 \pm 0.0008$. The values of ν and p_c obtained in this analysis are in good agreement with those found in the analysis of the susceptibility. Deviations from the universal fit for large values of the scaling variable x are again due to corrections to scaling. In both scaling analyses for $r_c = 0.05$ we were unable to use data for $L < 30$ since correction terms to the simple scaling forms became important. Reasonable scaling plots of the susceptibility and the gel fraction were not possible for $r_c = 0.005$ because of the magnitude of the finite-size effects.

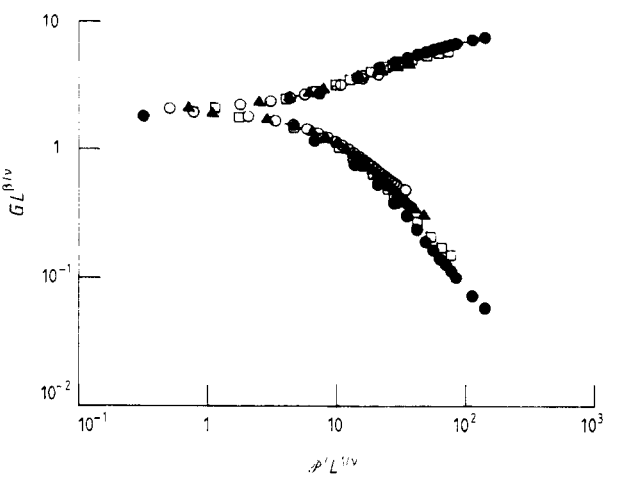

Figure 5. Finite-size scaling plot for the gel fraction G for $r_c = 0.05$, $p_c = 0.0852$, $\beta = 0.40$ and $\nu = 0.85$. Curves are shown for several values of L: 30(○), 40(▲), 60(□) and 100(●).

The ratio of critical amplitudes $R = C^-/C^+$ for the susceptibility, which has been shown to be a universal quantity in percolation [18], is also estimated from figure 4 by measuring the vertical distance between the two parallel lines drawn through the asymptotic regions above and below p_c. From this procedure, we find the critical amplitude ratio to be $R = 5.1 \pm 0.9$. This value is markedly different from the percolation value between 8 and 11 which suggests that our model may be in a different universality class than percolation.

3.2. Cluster size distributions

The distribution in the number of clusters n_s of size s has been investigated as a function of s and p. Figure 6 shows a monotonic decrease in n_s plotted against s for creation rate $r_c = 0.05$ and p near the gel point p_c. This monotonic decrease in n_s with

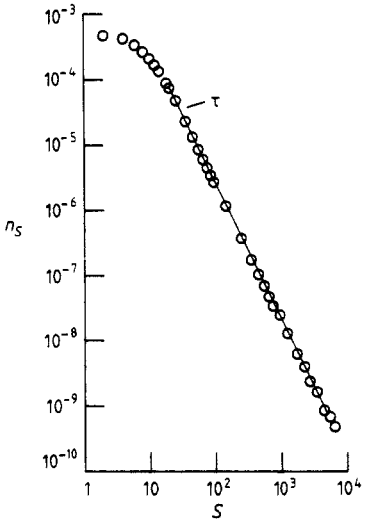

Figure 6. Cluster size distribution n_s at p_c for $r_c = 0.05$, $L = 100$. Data are averaged over several cluster sizes with ordinate values taken as a geometric mean. The slope of the straight line has the value $\tau = 2.1 \pm 0.1$.

s is seen for all values of p, which is the same qualitative behaviour found in percolation [13]. Similar monotonic behaviour is observed for creation rate $r_c = 0.005$ as shown in figure 7. Striking differences, however, are seen between the monotonic behaviour

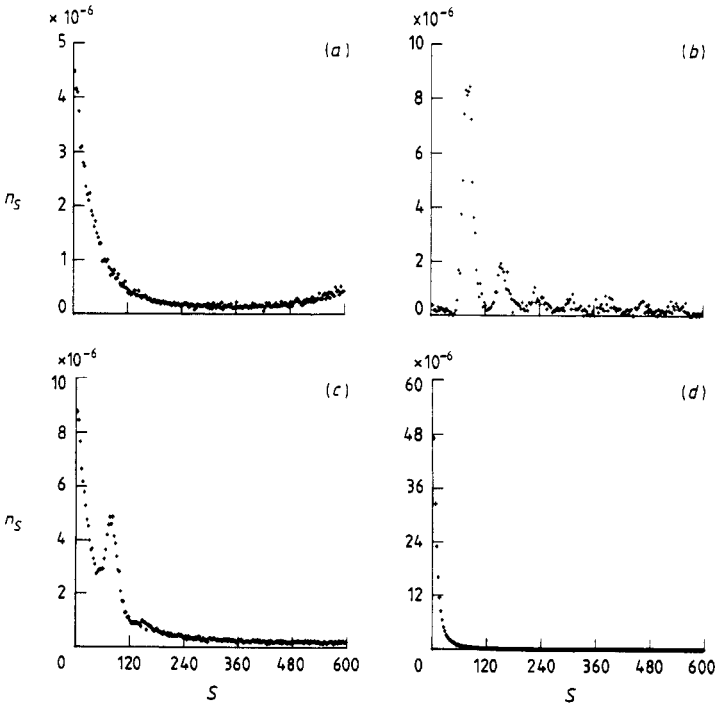

Figure 7. Cluster size distribution n_s at p_c for $L = 20$ with (*a*) $r_c = 0.005$, $c_1 = 0.0$; (*b*) $r_c = 0.0$, $c_1 = 0.0003$; (*c*) $r_c = 0.005$, $c_1 = 0.0003$ and (*d*) $r_c = 0.05$, $c_1 = 0.0003$.

in our model and the oscillatory distributions observed in a similar gelation model [11]. In that model, initiators are only created at the start of the growth process with concentration c_1, and the observed oscillations in the cluster distributions, which are shown in figure 7, are due to the joining of clusters of a characteristic size s^* to produce larger clusters whose sizes are a multiple of the characteristic size. Since new clusters are being formed at every stage of the growth process in our model, there will be no characteristic size emerging from the growth, i.e. $s^* = 1$.

Figure 7 also shows the effect of starting the growth process with an initial concentration c_1 of initiators and allowing new initiators to be created with rate r_c. For $r_c = 0.005$ and $c_1 = 0.0003$, one can still observe a characteristic peak in the cluster distributions at the gel point, although most of the oscillations have been damped out by the creation of new initiators. No characteristic size can be seen at p_c when $r_c = 0.05$ and $c_1 = 0.0003$.

According to (9), the cluster distribution n_s exhibits power-law behaviour as a function of s at the gel point, i.e. $n_s \sim s^{-\tau}$ for $p = p_c$ and $s \to \infty$. This behaviour corresponds to the linear region, spanning more than two and one-half decades, observed in the log-log plot of n_s against s (figure 6). The slope of the linear region yields a droplet exponent $\tau = 2.1 \pm 0.1$ which agrees with percolation values [19]. Attempts were made to scale the cluster distributions for $r_c = 0.05$ using the droplet scaling form giving in (9). These attempts, however, were unsuccessful for a wide range of values for σ, τ and p_c, including the droplet exponents $\sigma = 0.48$ and $\tau = 2.1$ found for percolation (see figure 8).

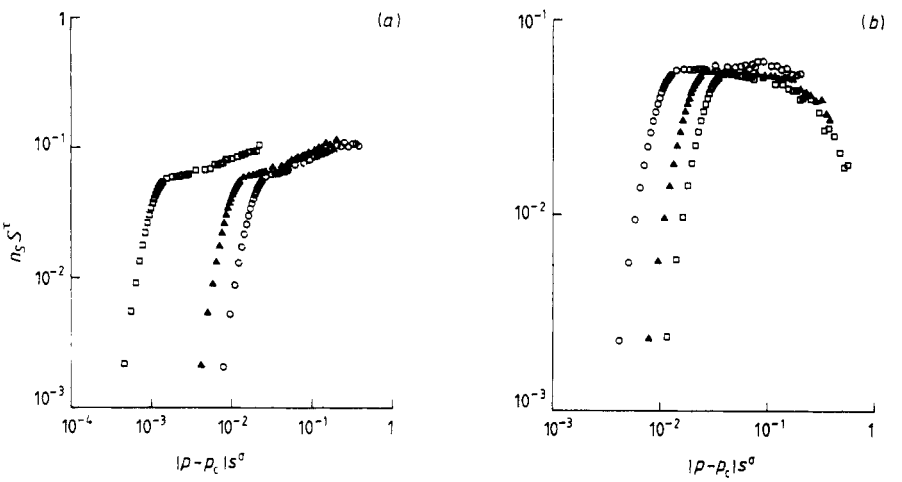

Figure 8. Droplet scaling plots for the cluster size distribution with $r_c = 0.05$, $p_c = 0.0850$, $\tau = 2.2$, $\sigma = 0.48$. (*a*) Scaling for $p < p_c$, curves are shown for $p = 0.0773$(○), $p = 0.0880$(▲) and $p = 0.0827$(□). (*b*) Scaling for $p > p_c$, curves are shown for $p = 0.0880$(○), $p = 0.0907$(▲) and $p = 0.0933$(□).

The cluster distributions were successfully scaled using a modified scaling form given by

$$n_s = s^{-\tau} \exp[-(Bs^{\sigma} + A)|p - p_c|]h(s) \tag{12}$$

where σ and τ are the universal, droplet exponents and A and B are non-universal constants. This form reproduces the correct asymptotic behaviour for the susceptibility

when inserted into (10) and is the same form that was used in a previous gelation study [11] with $s^* = 1$. Modified scaling plots of the cluster data above and below p_c for creation rate $r_c = 0.05$ are shown in figure 9. Percolation droplet exponents $\sigma = 0.48$ and $\tau = 2.1$ were used and the parameters A, B, and p_c were varied to produce optimal fits for the scaled data.

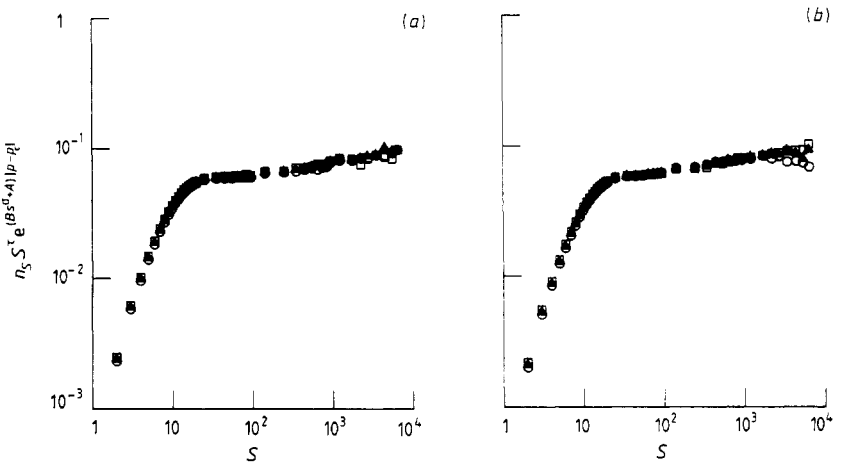

Figure 9. Modified scaling plots for the cluster size distribution with $r_c = 0.05$, $p_c = 0.0850$, $\tau = 2.2$, $\sigma = 0.48$. (*a*) Scaling for $p < p_c$ with $A = -5.0$, $B = -1.0$, curves are shown for $p = 0.0880(\bigcirc)$, $p = 0.0907(\blacktriangle)$ and $p = 0.0933(\square)$. (*b*) Scaling for $p > p_c$ with $A = 0.0$, $B = 3.0$, curves are shown for $p = 0.0773(\bigcirc)$, $p = 0.0800(\blacktriangle)$ and $p = 0.0827(\square)$.

4. Conclusions

We have used finite-size scaling analyses of the bulk properties to obtain estimates for the critical exponents β, γ and ν and the critical amplitude ratio $R = C^-/C^+$ for initiator creation rate $r_c = 0.05$. The critical exponents are, to within error bars, the same as those found in percolation and other kinetic gelation studies. Our best estimate for R is different to the 'universal' percolation value and is consistent with other kinetic gelation values. Reasonable scaling plots were not possible for creation rate $r_c = 0.005$ because of the strong finite-size effects. The shape of the cluster size distributions in our model are qualitatively the same as those seen in percolation, but they are strikingly different from the oscillatory behaviour observed in other kinetic gelation models. Analyses of these distributions, however, indicate that the scaling form which works well for percolation does not work well for this model. A modified scaling form, which works for other gelation models, produces good fits for cluster data above and below the gel point. Although the creation of initiators with rate r_c does affect the shape of the cluster distributions, it does not alter the critical behaviour observed in kinetic gelation. Our results, however, do support the conclusion drawn by other gelation studies: namely, that kinetic gelation appears to be in a different universality class to percolation.

Acknowledgments

This research was supported in part by National Foundation Grant no DMR-8715740.

References

[1] Flory P J 1941 *J. Am. Chem. Soc.* **63** 3083, 3091, 3096
[2] Stockmayer W H 1943 *J. Chem. Phys.* **11** 45
[3] de Gennes P G 1976 *J. Physique Lett.* **37** 11
[4] Stauffer D 1976 *J. Chem. Soc. Faraday Trans.* II **72** 1354; 1978 *Phys. Rev. Lett.* **41** 1333
Stauffer D, Coniglio A and Adam M 1982 *Adv. Polymer Sci.* **44** 103
[5] Manneville P and de Seze L 1981 *Numerical Methods in the Study of Critical Phenomena* ed I Della Dora, J. Demongeot and B. Lacolle (Berlin: Springer)
[6] Herrmann H J, Landau D P and Stauffer D 1982 *Phys. Rev. Lett.* **49** 412
Herrmann H J, Stauffer D and Landau D P 1983 *J. Phys. A: Math. Gen.* **16** 1221
[7] Pandey R B 1984 *J. Stat. Phys.* **34** 163
[8] Matthews-Morgan D, Landau D P and Herrmann H J 1984 *Phys. Rev.* B **29** 6328
[9] Bansil R, Herrmann H J and Stauffer D 1984 *Macromolecules* **17** 998; 1985 *J. Polymer Sci. Polym. Symp.* **73** 175
[10] Jan N, Lookman T and Stauffer D 1983 *J. Phys. A: Math. Gen.* **16** L117
[11] Ashvin Chhabra, Matthews-Morgan D, Landau D P and Herrmann H J 1984 *Kinetics of Aggregation and Gelation* ed F Family and D P Landau (Amsterdam: North-Holland) p 43; 1985 *J. Phys. A: Math. Gen.* **18** L575; 1986 *Phys. Rev.* B **34** 4796
[12] Herrmann H J 1986 *Phys. Rep.* **136** 155
[13] Flammang A 1977 *Z. Phys.* B **28** 47
[14] Tanford C 1961 *Physical Chemistry of Macromolecules* (New York: Wiley)
[15] Fisher M E 1971 *Critical Phenomena* ed M S Green (New York: Academic) p 1
[16] Essam J W and Fisher M E 1963 *J. Chem. Phys.* **38** 802
Fisher M E 1967 *Physics* **3** 255
[17] Heermann D W and Stauffer D 1981 *Z. Phys.* B **44** 339
Margolina A, Herrmann H J and Stauffer D 1982 *Phys. Lett.* **93A** 73
[18] Aharony A 1980 *Phys. Rev.* B **22** 400
[19] Margolina A, Nakanishi H, Stauffer D and Stanley H E 1984 *J. Phys. A: Math. Gen.* **17** 1683
Rapaport D C 1985 *J. Phys. A: Math. Gen.* **18** L175